

SCIENTIFIC REPORTS



OPEN

High frequency abrupt shifts in the Indian summer monsoon since Younger Dryas in the Himalaya

Sheikh Nawaz Ali¹, Jyotsna Dubey¹, Ruby Ghosh¹, M Firoze Quamar¹, Anupam Sharma¹, P Morthekai¹, A P Dimri², Mayank Shekhar¹, Md. Arif¹ & Shailesh Agrawal¹

In order to quantify the Indian summer monsoon (ISM) variability for a monsoon dominated agrarian based Indian socio-economy, we used combined high resolution $\delta^{13}\text{C}$, total organic carbon (TOC), sediment texture and environmental magnetic data of the samples from a ~3 m deep glacial outwash sedimentary profile from the Sikkim Himalaya. Our decadal to centennial scale records identified five positive and three negative excursions of the ISM since last ~13 ka. The most prominent abrupt negative ISM shift was observed during the termination of the Younger Dryas (YD) between ~11.7 and 11.4 ka. While, ISM was stable between ~11 and 6 ka, and declined prominently between 6 and 3 ka. Surprisingly, during both the Medieval Warm Period (MWP) and Little Ice age (LIA) spans, ISM was strong in this part of the Himalaya. These regional changes in ISM were coupled to southward shifting in mean position of the Intertropical Convergence Zone (ITCZ) and variations in East Asian monsoon (EAM). Our rainfall reconstructions are broadly in agreement with local, regional reconstructions and PMIP3, CSIRO-MK3L model simulations.

Indian summer monsoon (ISM) is a vital source of precipitation and significant component of Asian monsoon system and global climate. It originates by seasonal reversal of winds due to differential heating of the Indian sub-continent and Tibetan Plateau^{1–3}. By contributing over 80% of the total annual rainfall in India⁴, ISM significantly influences agrarian based Indian socio-economy and is considered as the most significant weather system nourishing the Himalayan glaciers^{5–7}. Abrupt shifts in the ISM on decadal to centennial scales might severely affect Indian socio-economy as observed in the recent past⁸ and is associated with the rise and fall of ancient human civilisations^{9–12}. In order to improve the predictive capabilities of the future ISM variability, characterization of the ISM precipitation before the instrumental period is becoming an urgent need. To understand the trends in the ISM variability, high resolution proxy records of precipitation with greater temporal and geographic coverage are necessary. Most of the records of the ISM variability during the Late Pleistocene to Holocene, when earth experienced several abrupt climatic shifts, are generated from marine archives primarily from Arabian Sea^{13–19} and Bay of Bengal^{20,21} while, from terrestrial archives high resolution data is scanty^{11,22–31} and is often suffering from age uncertainties. Therefore, ISM variability should be explored with a terrestrial high resolution monsoon proxy record with a greater temporal coverage to assess the inferred role of solar forcing^{16–18}, teleconnections to North Atlantic climate changes^{13,16} and variations in the East Asian monsoon (EAM)²¹ prior to the last glacial and Holocene. The Himalaya, an underexplored yet significant region acting as one of the ‘modulators of the ISM’ together with the Tibetan Plateau (TP), is the better, if not ideal region for quantifying past ISM variability. Although, some work has been done in the eastern Indian Himalaya, however, most of the records are qualitative and showed incongruity (Fig. S1). The climatologically sensitive transitional zone lying between the dry Trans Himalaya/Tibet towards north and the sub-humid Himalaya towards south that receives high precipitation (amplified signal) during intensified ISM and vice-versa is most suitable in this regard (Fig. 1). Our study area, the Chopta valley, a proglacial outwash plain in north Sikkim Himalaya fulfills the erstwhile conditions (Figs 1 and 2). Here we present a high resolution carbon isotope signature ($\delta^{13}\text{C}$) preserved in sediment organic matter (SOM) of Chopta valley combined with total organic carbon (TOC), sediment texture and environmental magnetic data to document the ISM variability in the last ~13 ka (Fig. 3), which also helped unraveling the forcing factors responsible for ISM variability. To explore the link between ISM variability with northern high latitude climate

¹Birbal Sahni Institute of Palaeosciences, Lucknow, India. ²School of Environmental Sciences, Jawaharlal Nehru University, New Delhi, India. Correspondence and requests for materials should be addressed to S.N.A. (email: snawazali@gmail.com) or S.A. (email: as.shail@gmail.com)

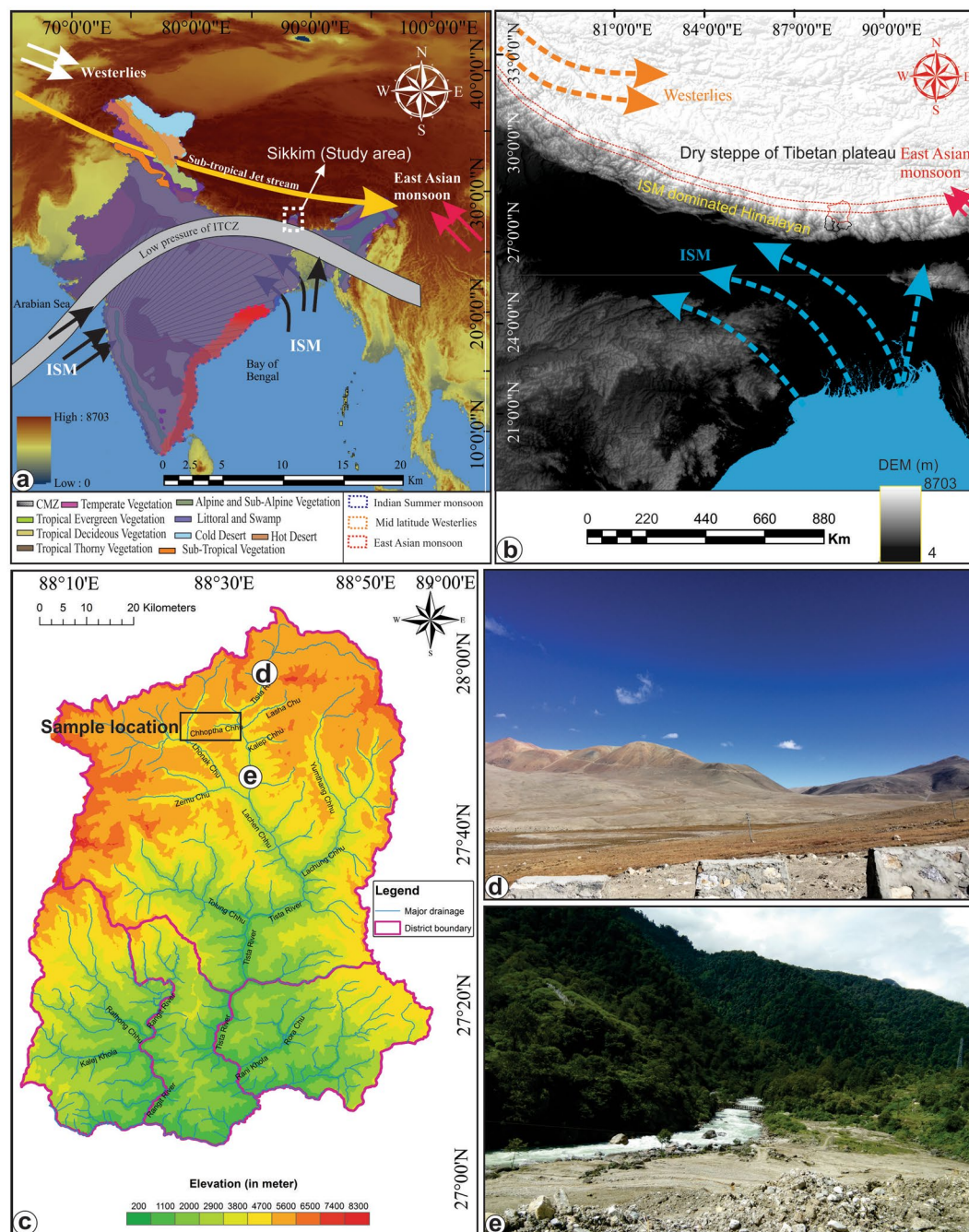


Figure 1. Map compilation showing (a) the location of the study area i.e. the Sikkim Himalaya in India with different vegetation zones and weather systems (modified after Dixit & Tandon⁷¹ and Zorzi *et al.*⁷²); (b) shuttle radar topographic mission (SRTM) digital elevation model (DEM) of central and eastern parts of India showing the study area, Sikkim (outlined in red) and the approximate transitional zone between the dry steppe of the trans-Himalaya towards the north and the sub-humid Himalaya to the south (marked between two red dashed lines); (c) Digital elevation model showing the major drainage and the location of sampling sites; (d) Dry steppe vegetation towards the north of the sampling sites. Location of the photographs is shown in Fig. 1c. (The maps are created using ArcGIS Version 10.2) and (e) Field photograph showing sub humid vegetation towards south of sampling sites.

changes during the last deglaciation, we have compared our data with regional marine, speleothem and global ice core records. The model simulation outputs are giving significantly comparable results. The model study is also performed to see spatial extent of ISM during past climate change scenario.

$\delta^{13}\text{C}$ and Total Organic Carbon (TOC) content in SOM and bulk sediment κ_{if} . The $\delta^{13}\text{C}$ values in the SOM are significantly used as a climate proxy for regional precipitation given that the organic matter source

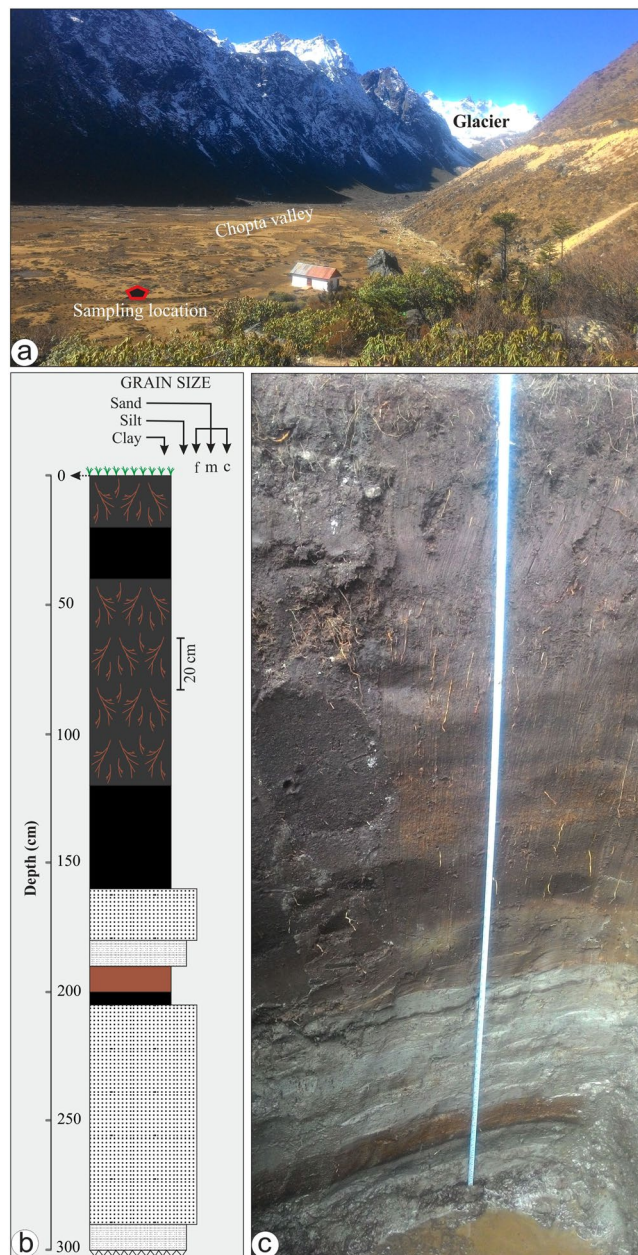


Figure 2. (a) Field photograph taken facing upstream direction, showing the synoptic view of the Chopta valley. The red pentagon shows the sampling location. (b) Detailed litholog of the sedimentary profile. (c) Field photograph showing the texture of the sedimentary profile.

is C_3 plants^{32–36} (see supplementary data for details). From the variations observed in TOC content of the profile, it is observed that the detrital input (glacial sediments) and environmental factors have significantly affected the TOC content of the profile³⁵. The lower half of the sediment profile (~300 to 160 cm; ~12 to 10 ka) having coarse lithology and high sedimentation rate show very low TOC with a couple of high excursions. However, the upper half of the profile (~160 to top; 10 ka to present) has high TOC suggesting a homogenised and favorable environment for floral growth and organic matter preservation (Figs 2 and 3).

To understand the isotopic response of the vegetation towards rainfall, we have generated a modern analogue using SOM of surface samples. The $\delta^{13}C$ values of SOM of the Chopta valley vary between -25.8 and -27.7‰ (average -26.6‰) showing little variation and suggesting an overall dominance of C_3 plants. Moreover, it has also been observed that the $\delta^{13}C$ values do not exhibit any significant trend between the hill slope and valley floor samples suggesting an isotopically homogenized system³⁷. The $\delta^{13}C$ values used to quantify the present day precipitation using the equations proposed by Kohn *et al.*³⁸ and Basu *et al.*³⁹ are in agreement and verified with CRU TS 3.24 data⁴⁰. The $\delta^{13}C$ values of de-carbonated samples in a ~3 m deep sedimentary profile vary between -28.0 and -24.3‰ having a significant difference of 3.7‰ (mean value -26.7‰) (Fig. 3; Table S1). Chronology of deposition for the Chopta valley profile is developed using a Bayesian age model using five ^{14}C AMS radiocarbon

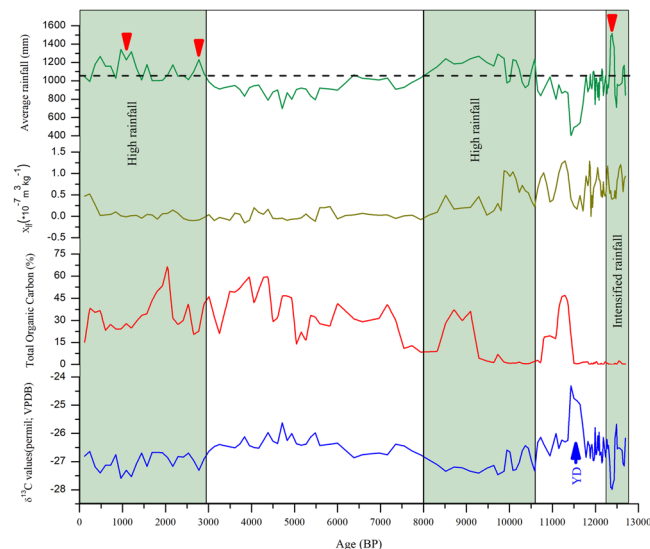


Figure 3. Measured $\delta^{13}\text{C}$ value (‰; VPDB; blue line), total organic carbon (TOC; %; red line) and low field magnetic susceptibility ($10^{-7}\text{m}^3\text{kg}^{-1}$; olive green line) of the sedimentary profile are shown against the depositional age (BP; ^{14}C AMS). The top green line shows the average reconstructed palaeoprecipitation values (mm) based on the $\delta^{13}\text{C}$ values using empirical relationship given in Kohn³⁸ and Basu *et al.*³⁹.

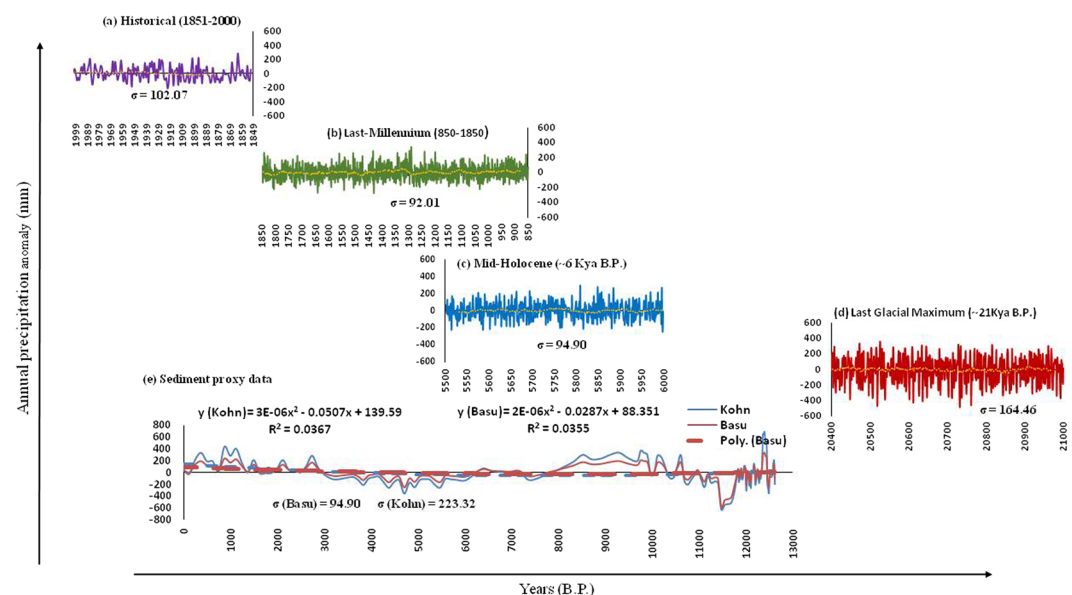


Figure 4. (a) Variations of annual rainfall anomaly (mm) averaged over core monsoon region ($73\text{--}82^\circ\text{E}$; $18\text{--}28^\circ\text{N}$) during (a) Historical (1850–2005), (b) Last Millennium (850–1849), (c) Mid-Holocene (~ 6 kya before present (B.P.) and (d) Last Glacial Maximum (LGM; ~ 21 kya B.P.) over Indian region from IPSL-CM5A-LR for (a), CSIRO-Mk3L for (b) and (c) and COSMOS-ASO for (d) global climate models respectively. For Mid-Holocene and Last glacial maximum variations are shown over a period of 500 and 600 years respectively. For each period, σ represents the standard deviation over the years while the line curves show the 33 years moving average over that period. (e) Precipitation record derived from proxy sediment core data from two locations in the Upper Sikkim valley where dashed line in corresponding colors with y-x equation represents the second degree polynomial regression fit. The inter-annual variability of rainfall gradually decreased from last glacial maximum to historical as is clearly evident from σ value.

dates. The magnetic susceptibility (MS) shows a definite fluctuating trend reflecting lithological changes throughout the profile. The sandy horizons show maximum MS values while the organic peaty layers have minimum MS values (Supplementary Information 1).

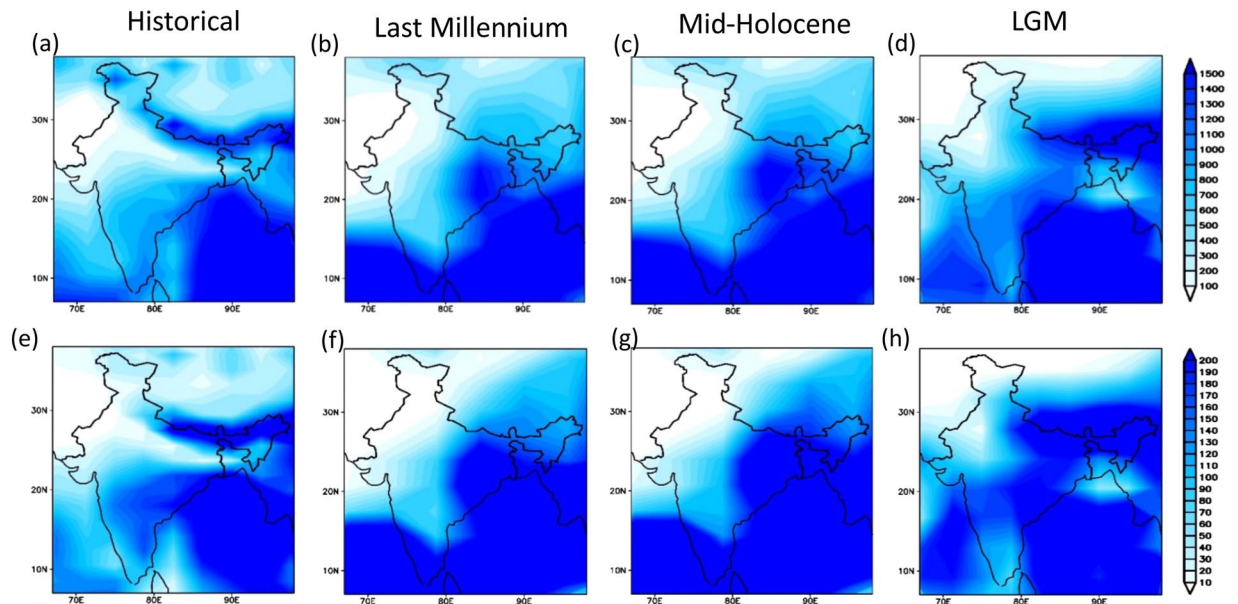


Figure 5. Variations of Annual precipitation climatology (mm) (a–d) and JJAS precipitation climatology (mm/month) (e–h) over Indian sub-continental region (67–98°E; 7–38°N) during (a,e) Historical (1850–2005), (b,f) Last Millennium (850–1849), (c,g) Mid-Holocene (~6 kya B.P.) and (d,h) Last Glacial Maximum (LGM; ~21 kya B.P.) from IPSL-CM5A-LR for (a,e), CSIRO-Mk3L for (b,f) and (c,g) and COSMOS-ASO for (d,h) global climate models respectively. For Mid-Holocene and Last glacial maximum variations are shown over a period of 500 and 600 years respectively.

Palaeo-precipitation reconstruction and correlation. Unlike the western and central Himalaya, dominated by extra-tropical westerlies during the winters, the Eastern Himalaya is affected by the thermal gradient between the Bay of Bengal and Indian subcontinent^{41,42} and is dominated by the ISM precipitation. Although the amount of rainfall keeps on decreasing from south to north across the Himalaya, however, the transitional zones receive good amount of rainfall during intensified ISM, making them ideal place to study ISM variability.

Here we present a quantitative data for the ISM variability deduced through carbon isotopic data of SOM following Kohn *et al.*³⁸ and Basu *et al.*³⁹ (Fig. 3) in the last ~12.7 ka from a sediment profile mentioned above (Figs 2 and 3). It is observed that during the Pleistocene–Holocene transition, the ISM witnessed abrupt high frequency fluctuations^{16–19,21}. Our combined data show that during the entire span of the Younger Dryas (YD) stadial between ~12.7 and 11.6 ka, the ISM was weaker than now, but around 12.4 ka an abrupt positive centennial scale excursion (~42% increase in rainfall) has been noticed, possibly the most wettest one within the last deglacial period. The most pronounced and abrupt weakening (~63% drop in rainfall) in the ISM has been observed at the termination of the YD between ~11.7 and 11.4 ka. Subsequently, a gradual rising trend for the ISM is noticed until ~10.6 ka, but still with lower rainfall than present. The overall weak ISM between ~12.7 and 11.6 ka may be attributed to the weakening of the Atlantic Meridional Overturning Circulation (MOC) that occurred during the YD⁴¹. Furthermore, central and eastern Himalayan glaciers showed a short term advancement during this period, that has been attributed to lower temperature^{42–44}. Being in the domain of ISM we believe that the glaciers advanced due to lower temperatures during the YD that sustained and nourished by the wet early Holocene. Similar weakening in the ISM during the YD is observed by other workers also^{18,19,21,44–47}. Our estimation shows that the rainfall dropped to a minimum of ~400 mm at the termination of the YD with a deficit of ~650 mm from normal. The YD, characterized by weak ISM and strengthened westerlies^{22,48,49}, is a canonical abrupt climatic event that has been linked to marked reduction in the North Atlantic meridional overturning circulation (MOC), and a shutdown or weakening of the MOC^{41,50–52}. Further, some recent records inferred that ISM precipitation was linked to variations in both the North Atlantic climate and EAM on multicentennial to millennial time scales^{18,22,53}. The increase in latitudinal thermal gradient drove stronger westerly winds during the YD cold span, and southward shift in mean position of ITCZ led to weakening of both the ISM and EAM⁵³. It is assumed that there is little influence of Western disturbances (WD) or westerly's on the Eastern Himalaya, however, a centennial scale abrupt strengthening in ISM between ~12.4 and 12.3 ka within the YD is surprising (Fig. 3). This abrupt strengthening in ISM might be due to interaction of WDs with a break in the summer monsoon trough which might have led to heavy rainfall for a brief spell in the Eastern Himalaya⁵⁴.

Gradual strengthening of the ISM after the YD glacial cooling event is recorded and is punctuated by two centennial to millennial scale precipitation minima phases during ~10.6–8.0 ka. It is observed that during this phase an increase of up to ~21% in ISM precipitation is witnessed. Recently, Bhushan *et al.*⁵⁵ also inferred a similar gradual strengthening of ISM after the YD from monsoon dominated central Himalaya using detrital proxies. Post YD strengthening of ISM has been documented in both marine and terrestrial proxies on regional scale^{14,15,19,20,22,45,48,56–61} (Fig. S3). The early Holocene ISM intensification has been attributed to two inherently

related different processes namely boreal summer insolation considered as the external forcing mechanism^{15,62} and significant reduction in albedo due to decrease in Tibetan Plateau snow cover⁶³. The strong and stable ISM (~10.6–8.0 ka) is followed by a gradual decline during ~8 to 3 ka and is punctuated by a moderate ISM event recorded at ~6.4 ka (Fig. 2). It is observed that there has been a slight fluctuation in the precipitation between ~8 and 6 ka and is followed by a gradual decrease in precipitation that persisted until ~3 ka.

Our observations broadly corroborate with the inferences of a moderate surface runoff⁵⁵ from a similar ISM dominated region from the Central Himalaya. The gradual fluctuating trend seen in the ISM precipitation post ~8 ka is also accorded by coupled atmosphere-ocean parameters used in global climate model simulations⁶⁴. Further, our data is also in correspondence with that of ocean data sets suggesting similar ocean-atmospheric conditions relative to present and matches well even with the mid-Holocene period (ca. 6000 yrs BP)^{65,66}. The fluctuating decreasing trend in the rainfall pattern post ~6 ka is attributed to the progressive decrease in insolation and south ward shift of the ITCZ after mid Holocene. Stabilization of ISM took place after ~3 ka and is broadly punctuated by three enhanced ISM events at ~2.8 ka (15%), 2.1 ka (10%) and during 1300 – 400 (26%) yr BP. The sharp fluctuating trend with rainfall reaching to its maximum (~26% above normal) during ~1300 to 400 yrs BP corresponding to Medieval warm period (MWP), an intensified and wet ISM phase^{40,67}. It is also inferred that after ~300 yrs BP (Little Ice age) amelioration in the ISM is recorded and corroborates well with tree ring based records of Shekhar *et al.*⁶⁸. Surprisingly our data show no drop in ISM precipitation during the LIA in the Sikkim Himalaya attributable to the dual interactions of ITCZ and strong WDs^{61,69} during this phase. A high frequency of monsoon break events during ~1400 and 1700 AD might have cumulatively generated centennial-scale episodes of negative precipitation anomalies over central India and positive precipitation anomalies over northeast India⁷⁰. Sinha *et al.*⁷⁰ inferred influence of planetary-scale ITCZ changes on ISM precipitation by modulating the frequency of active-break periods which is further corroborated by our results.

Our $\delta^{13}\text{C}$ based palaeoprecipitation reconstruction from the eastern Himalaya is in great agreement with the regional terrestrial and marine palaeorecords as well as with those of glacial reconstructions from the adjoining areas. It is evident from our data that during the Pleistocene-Holocene boundary the ISM was very unstable. The broad correlation between different proxy data sets suggests common forcing factors that need to be further understood by generating high resolution palaeoprecipitation data sets from ecologically diverse climatic regions of the Indian subcontinent (Fig. S3). We show that the early phase of the Holocene has witnessed dramatic centennial to millennial scale abrupt precipitation fluctuations. Although, qualitative reconstructions suggest a marginally weak to moderate ISM during the mid-Holocene, however, it is now apparent from our study that the precipitation was marginally low with respect to present and punctuated by centennial scale dry spells (Fig. 3). Further, it is suggested that the area seems to have been under the influence of enhanced mid-latitude westerlies during the dry spells like YD and LIA. The model output shows gradual change in precipitation pattern from Last Glacial Maximum (LGM) to Historical (Figs 4 and 5). The variations in precipitation among LGM, mid Holocene and Historical periods are also clearly seen. As the model shows precipitation pattern shift over eastern to western Himalaya from mid Holocene to Historical period, that also delineates the reconstruction of precipitation over western Himalaya after Indus valley civilization ruin.

References

- Halley, E. An historical account for the trade winds, and monsoons, observable in the seas between the Tropics, with an attempt to assign the physical cause of the said winds. *Philos. Trans. Roy. Soc. London* **16**, 153–168 (1686).
- Webster, P. J. The elementary monsoon. *Monsoons*, J. S. Fein and P. L. Stephens, Eds, John Wiley 3–32 (1987).
- Li, C. & Yanai, M. The onset and interannual variability of the Asian summer monsoon in relation to land–sea thermal contrast. *J. Climate* **9**, 358–375 (1996).
- Gadgil, S. The Indian Monsoon, GDP and agriculture. *Econom. Pol. Weekly* **41**, 4887–4895 (2006).
- Finkel, R. C. *et al.* Beryllium-10 dating of Mount Everest moraines indicates a strong monsoon influence and glacial synchronicity throughout the Himalaya. *Geology* **31**, 561–564 (2003).
- Yang, B. *et al.* Late Holocene monsoonal temperate glacier fluctuations on the Tibetan Plateau. *Global and Planetary Change* **60**, 126–140 (2008).
- Ali, N. S. & Juyal, N. Chronology of late quaternary glaciations in Indian Himalaya: a critical review. *J. Geol. Soc. India* **82**, 628–638 (2013).
- Emergency Disasters Data Base [EM-DAT]. <http://www.emdat.be>.
- Witzel, M. In *India and the Ancient world. History, Trade and Culture before A.D. 650. P.H.L. Eggermont Jubilee Volume*, G. Pollet, Ed. (Orientalia Lovaniensia Analecta Leuven, 253–213 (1987).
- Witzel, M. In *Aryans and Non-Aryans, Evidence, Interpretation and Ideology* (Cambridge: Harvard Oriental Series: Opera Minora, 3, 337–404 (1999).
- Prasad, S. *et al.* Prolonged monsoon droughts and links to Indo-Pacific warm pool: a Holocene record from Lonar Lake, central India. *Earth Planet. Sci. Lett.* **391**, 171–182, <https://doi.org/10.1016/j.epsl.2014.01.043> (2014).
- Sarkar, A. *et al.* Oxygen isotope in archaeological bioapatites from India: implications to climate change and decline of Bronze Age Harappan civilization. *Sci. Rep.* **6**, 26555, <https://doi.org/10.1038/srep26555> (2016).
- Schulz, H., von Rad, U. & Erlenkeuser, H. Correlation between Arabian Sea and Greenland climate oscillations of the past 110,000 years. *Nature* **393**, 54–57 (1998).
- Sirocko, F. *et al.* Century-scale events in monsoonal climate over the past 24,000 years. *Nature* **364**, 322–324, <https://doi.org/10.1038/364322a0> (1993).
- Overpeck, J. T., Anderson, D. M., Trumbore, S. & Prell, W. L. The southwest Indian monsoon over the last 18,000 years. *Clim. Dyn.* **12**, 213–225, <https://doi.org/10.1007/BF00211619> (1996).
- Gupta, A. K., Anderson, D. M. & Overpeck, J. T. Abrupt changes in the Asian south west monsoon during the Holocene and their links to the North Atlantic Ocean. *Nature* **421**, 354–356, <https://doi.org/10.1038/nature01340> (2003).
- Gupta, A. K., Das, M. & Anderson, D. M. Solar influence on the Indian summer monsoon during the Holocene. *Geophys. Res. Lett.* **32**, L17703, <https://doi.org/10.1029/2005GL022685> (2005).
- Gupta, A. K. *et al.* Solar forcing of the Indian summer monsoon variability during the Ållerød period. *Science Reports* **3**, 2753, <https://doi.org/10.1038/srep02753> (2013).
- Kessarkar, P. M. *et al.* Variation in the Indian summer monsoon intensity during the Bølling-Ållerød and Holocene. *Paleoceanography* **28**, 413–425 (2013).

20. Govil, P., Naidu, P. D. & Kuhnert, H. Variations of Indian monsoon precipitation during the last 32 kyr reflected in the surface hydrography of the western Bay of Bengal. *Quat. Sci. Rev.* **30**, 3871–3879 (2011).
21. Rashid, H., England, E., Thompson, L. & Polyak, L. Late glacial to Holocene Indian summer monsoon variability based upon sediment. *Terr. Atmos. Ocean. Sci.* **22**, 215–228 (2011).
22. Sinha, A. *et al.* Variability of southwest Indian summer monsoon precipitation during the Bølling-A^o llerød. *Geology* **33**, 813–816 (2005).
23. Sinha, A. *et al.* A 900 year (600 to 1500 AD) record of the Indian Summer Monsoon precipitation from the core monsoon zone of India. *Geophys. Res. Lett.* **34**, L16707, <https://doi.org/10.1029/2007GL030431> (2007).
24. Yadava, M. G. & Ramesh, R. Monsoon reconstruction from radiocarbon dated tropical Indian speleothems. *Holocene* **12**, 48–59 (2005).
25. Clift, P. D. & Plumb, R. A. *The Asian Monsoon: Causes, History and Effects*. Cambridge University Press 978-0-521-84799-5 270 (2008).
26. Berkelhammer, M., Sinha, A., Mudelsee, M. & Cannariato, K. G. Persistent multidecadal power in the Indian Summer Monsoon. *Earth Planet. Sci. Lett.* **290**, 166–172, <https://doi.org/10.1016/j.epsl.2009.12.017> (2010).
27. Ghosh, R. *et al.* A ~50 ka record of monsoonal variability in the Darjeeling foothill region, eastern Himalayas. *Quat. Sci. Rev.* **114**, 100–115 (2015).
28. Ghosh, R. *et al.* A modern pollen–climate dataset from the Darjeeling area, eastern Himalaya: Assessing its potential for past climate reconstruction. *Quaternary Science Reviews* **174**, 63–79 (2017).
29. Yadav *et al.* Recent wetting and glacier expansion in the northwest Himalaya and Karakoram. *Sci. Rep.* **7** <https://doi.org/10.1038/s41598-017-06388-5> (2017).
30. Rawat, S., Gupta, A. K., Sangode, S. J., Srivastava, P. & Nainwal, H. C. Late Pleistocene–Holocene vegetation and Indian summer monsoon record from the Lahaul, Northwest Himalaya, India. *Quat. Sci. Rev.* **114**, 167–181 (2015).
31. Agrawal, S. *et al.* Stable ($\delta^{13}\text{C}$ and $\delta^{15}\text{N}$) isotopes and magnetic susceptibility record of late Holocene climate change from a lake profile of the northeast Himalaya. *J. Geol. Soc. India* **86**, 696–705 (2015).
32. O’Leary, M. H. Carbon isotope fractionation in plants. *Phytochemistry* **20**(4), 553–567 (1981).
33. Farquhar, G. D., O’leary, M. H. & Berry, J. A. On the relationship between carbon isotope discrimination and the intercellular carbon dioxide concentration in leaves. *Funct. Plant Biol.* **9**(2), 121–137 (1982).
34. Zhang, J. *et al.* Holocene monsoon climate documented by oxygen and carbon isotopes from lake sediments and peat bogs in China: a review and synthesis. *Quat. Sci. Rev.* **30**(15), 1973–1987 (2011).
35. Rao, Z. *et al.* Relationship between the stable carbon isotopic composition of modern plants and surface soils and climate: a global review. *Earth Sci. Rev.* **165**, 110–119 (2017).
36. Street, J. H., Anderson, R. S. & Paytan, A. An organic geochemical record of Sierra Nevada climate since the LGM from Swamp Lake, Yosemite. *Quaternary Science Reviews* **40**, 89–106 (2012).
37. Dubey, D. *et al.* Characteristics of modern biotic data and their relationship to vegetation of the Alpine zone of Chopta valley, North Sikkim, India: Implications for palaeovegetation Reconstruction. *Holocene* (2017).
38. Kohn, M. J. Carbon isotope compositions of terrestrial C3 plants as indicators of (paleo) ecology and (paleo) climate. *Proc. Natl. Acad. Sci. USA* **107**, 19691–19695 (2010).
39. Basu, S. *et al.* Carbon isotopic ratio of modern C₃–C₄ plants from the Gangetic Plain, India and its implications to paleovegetational reconstruction. *Palaeogeography, Palaeoclimatology, Palaeoecology* **440**, 22–32 (2015).
40. Polanski, S., Fallah, B., Befort, D. J., Prasad, S. & Cubasch, U. Regional moisture change over India during the past millennium: a comparison of multi-proxy reconstructions and climate model simulations. *Glob. Planet. Chang.* **122**, 176–185 (2014).
41. McManus, J. F., Francois, R., Gherardi, J. M., Keigwin, L. D. & Brown-Ledger, S. Collapse and rapid resumption of Atlantic meridional circulation linked to deglacial climate changes. *Nature* **428**, 834–837, <https://doi.org/10.1038/nature02494> (2004).
42. Meyer, M. C. *et al.* Holocene glacier fluctuations and migration of Neolithic yak pastoralists into the high valleys of northwest Bhutan. *Quaternary Science Reviews* **28**, 1217–1237 (2009).
43. Rupper, S., Roe, G. & Gillespie, A. Spatial patterns of Holocene glacier advance and retreat in central. *Asia. Quat. Res.* **72**, 337–346 (2009).
44. Sati, S. P. *et al.* Timing and extent of Holocene glaciations in the monsoon dominated Dunagiri valley (Bangni glacier), Central Himalaya, India. *J. Asian Earth Sci.* **91**, 125–136 (2014).
45. Rashid, H., Flower, B. P., Poore, R. Z. & Quinn, T. M. A ~25 ka Indian Ocean monsoon variability record from the Andaman Sea. *Quaternary Science Reviews* **26**, 2586–2597 (2007).
46. Anand, P., Elderfield, H. & Conte, M. H. Calibration of Mg/Ca thermometry in planktonic foraminifera from a sediment trap time series. *Paleoceanography* **18**, 1050, <https://doi.org/10.1029/2002PA000846> (2003).
47. Kudrass, H. R., Hofmann, A., Doose, H., Emeis, K. & Erlenkeuser, H. Modulation and amplification of climatic changes in the Northern Hemisphere by the Indian summer monsoon during the past 80 ky. *Geology* **29**, 63–66 (2001).
48. Wang, Y. J. *et al.* A high-resolution absolute-dated late Pleistocene monsoon record from Hulu Cave, China. *Science* **294**, 2345–2348 (2001).
49. Porter, S. C. & Zhisheng, A. Correlation between climate events in the North Atlantic and China during the last glaciation. *Nature* **375**, 305–308 (1995).
50. Wang, Z., Kuhlbrodt, T. & Meredith, M. P. On the response of the Antarctic Circumpolar Current transport to climate change in coupled climate models. *J. Geophys. Res.* **116**, <https://doi.org/10.1029/2010JC006757> (2011).
51. Broecker, W. S., Peteet, D. M. & Rind, D. Does the ocean–atmosphere system have more than one stable mode of operation? *Nature* **315**, 21–26 (1985).
52. Broecker, W. S. Does the trigger for abrupt climate change reside in the ocean or in the atmosphere? *Science* **300**, 1519–1522 (2003).
53. Sun, Y. B. *et al.* Influence of Atlantic meridional overturning circulation on the East Asian winter monsoon: *Nature Geoscience* **5**, 46–49, <https://doi.org/10.1038/ngeo1326> (2012).
54. Pisharoty, P. R. & Desai, B. N. Western disturbances and Indian weather. *Mausam* **7**, 333–338 (1956).
55. Bhushan, R. *et al.* High-resolution millennial and centennial scale Holocene monsoon variability in the Higher Central Himalayas. *Palaeogeography, Palaeoclimatology, Palaeoecology* **489**, 333–338 (2017).
56. Gasse, F. Hydrological changes in the African tropics since the Last Glacial Maximum. *Quat. Sci. Rev.* **19**, 189–211 (2000).
57. Fleitmann, D. *et al.* Holocene forcing of the Indian Monsoon recorded in a stalagmite from southern Oman. *Science* **300**, 1737–1739 (2003b).
58. Dutt, S. *et al.* Abrupt changes in Indian summer monsoon strength during 33,800 to 5500 years B.P. *Geophys. Res. Lett.* **42**, 5526–5532, <https://doi.org/10.1002/2015GL064015> (2015).
59. Yuan, D. X. *et al.* Timing, duration and transition of the last interglacial Asian Monsoon. *Science* **304**, 575–578 (2004).
60. Prasad, S. & Enzel, Y. Holocene paleoclimates of India. *Quat. Res.* **66**, 442–453 (2006).
61. Dixit, Y., Hodell, D. A. & Petrie, C. A. Abrupt weakening of the summer monsoon in northwest India ~4100 yr ago. *Geology* **42**, 339–342 (2014).
62. Kutzbach, J. E. & Street-Perrott, F. A. Milankovitch forcing of fluctuations in the level of tropical lakes from 18 to 0 kyr BP. *Nature* **317**, 130–134 (1985).

63. Marzin, C. & Braconnot, P. Variations of Indian and African monsoons induced by insolation changes at 6 and 9.5 kyr BP. *Clim. Dyn.* **33**, 215–231 (2009).
64. LeGrande, A. N. & Schmidt, G. A. Sources of Holocene variability of oxygen isotopes in paleoclimate archives. *Clim. Past* **5**, 441–455 (2009).
65. Mukherjee, P., Sinha, N. & Chakraborty, S. Investigating the dynamical behavior of the Intertropical Convergence Zone since the last glacial maximum based on terrestrial and marine sedimentary records. *Quaternary International* **443**, 49–57 (2016).
66. Lüthi, D. *et al.* High-resolution carbon dioxide concentration record 650,000–800,000 years before present. *Nature* **453**, 379–382, <https://doi.org/10.1038/nature06949> (2008).
67. Graham, N. E., Ammann, C. M., Fleitmann, D., Cobb, K. M. & Luterbacher, J. Support for global climate reorganization during the “Medieval Climate Anomaly”. *Clim. Dyn.* **37**, 1217–1245 (2011).
68. Shekhar, M. *et al.* Himalayan glaciers experienced significant mass loss during later phases of little ice age. *Scientific Reports* **7**, Article number: 10305. <https://doi.org/10.1038/s41598-017-09212-2> (2017).
69. Sinha, A. M. *et al.* The leading mode of Indian Summer Monsoon precipitation variability during the last millennium. *Geophys. Res. Lett.* **38**, L15703 (2011).
70. Sinha, A. *et al.* A global context for megadroughts in monsoon, Asia during the past millennium. *Quat. Sci. Rev.* **30**, 47–62 (2011).
71. Dixit, Y. & Tandon, S. K. Hydroclimatic variability on the Indian subcontinent in the past millennium: review and assessment. *Earth Sci. Rev.* **161**, 1–15 (2016).
72. Zorzi, C. *et al.* Indian monsoon variations during three contrasting climatic periods: the Holocene, HeinrichStadial 2 and the last interglacial-glacial transition. *Quat. Sci. Rev.* **125**, 50–60 (2015).

Acknowledgements

The authors are thankful to the Director, Birbal Sahni Institute of Palaeosciences, Lucknow, India for his constant support and providing infrastructural facilities. Special thanks are to the Forest department, Govt. of Sikkim, Dept. of Home, Govt. of Sikkim and the Indian Army, Sikkim for their help and providing necessary permissions during the field work. Thanks are also due to the field staff who have worked tirelessly in the harsh conditions during the field work. Financial support from DST, New Delhi is highly acknowledged (SR/DGH-89/2014). The authors appreciate the three anonymous reviewers for their valuable comments.

Author Contributions

S.N.A. conceptualised and designed the research and performed the sampling. S.N.A., J.D., M.A. and S.A. did the sample analysis. S.N.A., S.A., R.G. and M.F.Q. wrote the manuscript and materials and methods section with inputs from all the co-authors (A.S., P.M., M.S., A.P.D.).

Additional Information

Supplementary information accompanies this paper at <https://doi.org/10.1038/s41598-018-27597-6>.

Competing Interests: The authors declare no competing interests.

Publisher's note: Springer Nature remains neutral with regard to jurisdictional claims in published maps and institutional affiliations.



Open Access This article is licensed under a Creative Commons Attribution 4.0 International License, which permits use, sharing, adaptation, distribution and reproduction in any medium or format, as long as you give appropriate credit to the original author(s) and the source, provide a link to the Creative Commons license, and indicate if changes were made. The images or other third party material in this article are included in the article's Creative Commons license, unless indicated otherwise in a credit line to the material. If material is not included in the article's Creative Commons license and your intended use is not permitted by statutory regulation or exceeds the permitted use, you will need to obtain permission directly from the copyright holder. To view a copy of this license, visit <http://creativecommons.org/licenses/by/4.0/>.

© The Author(s) 2018